Metal–carbon vibrational modes as a probe of the *trans* influence in vinylidene and carbonyl rhodium(I) complexes

Damien Moigno,[a] Wolfgang Kiefer,*[a] Berta Callejas-Gaspar,[b] Juan Gil-Rubio[b] and Helmut Werner*[b]

[a] *Institut für Physikalische Chemie, Universität Würzburg, Am Hubland, D-97074 Würzburg, Germany. E-mail: wolfgang.kiefer@mail.uni-wuerzburg.de; Fax: + 49 931 888 6332; Tel: + 49 931 888 6330*

[b] *Institut für Anorganische Chemie, Universität Würzburg, Am Hubland, D-97074 Würzburg, Germany. E-mail: helmut.werner@mail.uni-wuerzburg.de; Fax: + 49 931 888 4623; Tel: + 49 931 888 5260*

Received (in Strasbourg, France) 11th May 2001, Accepted 7th August 2001
First published as an Advance Article on the web 17th October 2001

FT-Raman spectroscopy and density functional theory (DFT) calculations have been used to study the *trans* influence of ligands L in complexes of the general composition *trans*-[RhX(L)($P\textit{i}Pr_3$)$_2$], where X = F, Cl, Br, I, CH_3 and C≡CPh; L = $^{13}C{=}^{13}CH_2$, C=CHPh and CO. For the vinylidene compounds **1**–**10**, the sequence of the *trans* influence C≡CPh > CH_3 > I > Br > Cl > F has been derived from the order of the ν(Rh=C) wavenumbers. In the carbonyl halide complexes **11**–**14**, the sequence of the *trans* influence for the halide ligands is the same as for the related vinylidene halide derivatives. The *trans* influence of the ligands X is discussed in terms of both the σ-donor capabilities of these ligands and the electronic repulsion between the d electrons of rhodium and the lone pairs of X.

The changes in the wavenumber of the ν(CO) vibrational mode have often been used as an indirect probe to study the donor capabilities of the ligands coordinated to the metal center in transition-metal carbonyl complexes.[1–6] However, to the best of our knowledge, no such studies have been carried out using the ν(M–CO) mode, even though the metal–carbon stretching mode is expected to be sensitive to variations in the electronic density on the metal. This is true also for transition-metal carbene and carbyne complexes, for which very few vibrational studies have been reported.[7–16] Moreover, the assignment of the metal–carbon stretching mode in carbene and carbyne complexes is relevant because it is an easily available source of information about the bonding in these types of compounds. Recently, we reported that the bands corresponding to the ν(Rh=C) vibrational modes in the Raman and infrared spectra of the compounds *trans*-[RhF(=C=CH_2)($P\textit{i}Pr_3$)$_2$] and *trans*-[RhF(=$^{13}C{=}^{13}CH_2$)($P\textit{i}Pr_3$)$_2$] could be assigned with the help of isotopic substitution as well as DFT calculations.[17] The availability of a series of vinylidene and carbonyl complexes containing different ligands in the *trans* position to the isolelectronic vinylidene and CO ligands gave us the opportunity to study for the first time the influence of the *trans* ligand on the metal–carbon bond of vinylidene complexes and to compare the results of this study with those derived from the comparison of the ν(CO) modes.

In this work we present a study on the influence of various ligands X on the rhodium–carbon bond of square-planar vinylidene and carbonyl rhodium(I) complexes by using the wavenumber of the metal–carbon stretching modes as a probe for the weakening of the Rh=C bond. The compounds studied were *trans*-[RhX(=$^{13}C{=}^{13}CH_2$)($P\textit{i}Pr_3$)$_2$] with X = F (**1**), Cl (**2**), Br (**3**) and I (**4**); *trans*-[RhX(=C=CHPh)($P\textit{i}Pr_3$)$_2$] with X = F (**5**), Cl (**6**), Br (**7**), I (**8**), CH_3 (**9**) and PhC≡C (**10**); and *trans*-[RhX(CO)($P\textit{i}Pr_3$)$_2$] with X = F (**11**), Cl (**12**), Br (**13**) and I (**14**). The results are rationalized with the support of DFT calculations on model compounds in which the bulky $P\textit{i}Pr_3$ ligands are replaced by PMe_3.

Results

Vibrational spectroscopy

The low-wavenumber region of the FT-Raman spectra of complexes **1**–**4** is outlined in Fig. 1. The ν(Rh=^{13}C) mode has been assigned to a band in the range between 559 and 540 cm^{-1} on the basis of isotopic substitution and DFT calculations.[17] In the infrared spectra, the corresponding bands were of very low intensity. The wavenumber of the metal–carbon stretching mode decreases in the order F > Cl > Br > I.

A coupling between the ν(Rh=C) and ν(RhX) modes was observed in the computer-animated vibrational simulation for the model compounds *trans*-[RhX(=C=CH_2)(PMe_3)$_2$]. This coupling should increase from X = I to X = F because the ν(Rh=^{13}C) and ν(RhX) bands are closer to each other (Table 1), the maximum coupling being found for the fluoro complex.[1] A probe to test the degree of coupling is the change in position of the ν(RhF) band in *trans*-[RhF(=C=CH_2)-($P\textit{i}Pr_3$)$_2$] relative to its ^{13}C containing analog **1**. A great difference would indicate an extensive coupling of the metal–carbon and metal–fluorine stretching vibrations. However, the ν(RhF) band is shifted by only 4 cm^{-1} to lower wavenumbers in *trans*-[RhF(=$^{13}C{=}^{13}CH_2$)($P\textit{i}Pr_3$)$_2$] (**1**) compared to *trans*-[RhF(=C=CH_2)($P\textit{i}Pr_3$)$_2$], whereas the position of the ν(Rh=C) mode is 13 cm^{-1} lower in **1** compared with the non-labeled complex.[17] Although this shift is larger than the difference in ν(Rh=^{13}C) between compounds **1** and **2** ($\Delta\nu$ = 8 cm^{-1}), the effect of the coupling together with the effect of the increasing mass of the metal fragment [RhX($P\textit{i}Pr_3$)$_2$] in going from **1** to **4** provokes some ambiguity in the interpretation of the change in ν(Rh=^{13}C) along the series. Moreover, the results of the calculations performed (see below) suggest that the order of ν(Rh=^{13}C) reflects the order of the Rh=C bond strengths.

The complexes **1**, **2** and **4** display in their IR spectra a band in the range 1569–1582 cm^{-1} that was not observed in the FT-Raman spectra and is assignable to the vinylidenic

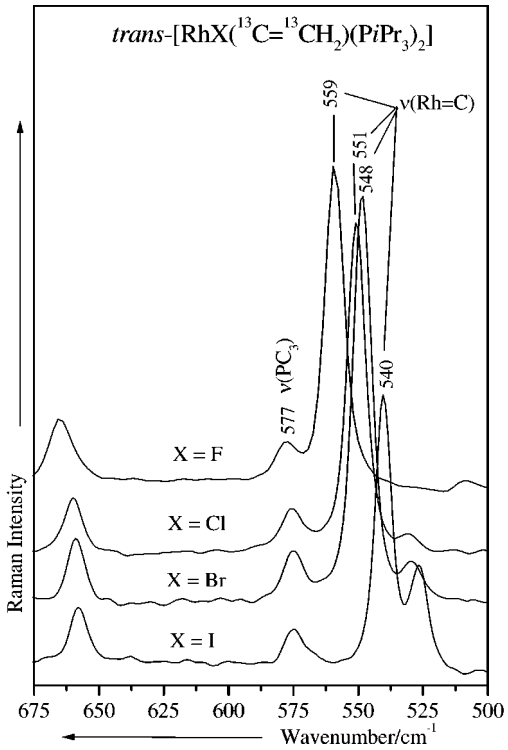

Fig. 1 The low-wavenumber region of the FT-Raman spectra of *trans*-[RhX(=^{13}C=^{13}CH$_2$)(P*i*Pr$_3$)$_2$] (X = F, Cl, Br, I).

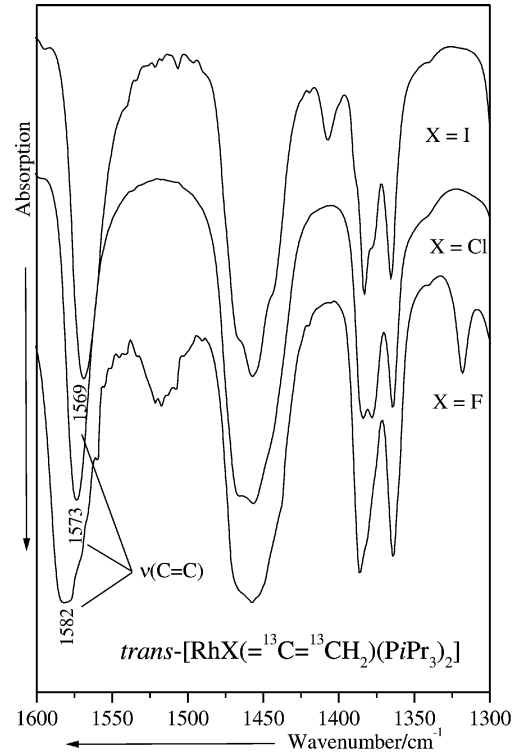

Fig. 2 The high-wavenumber region of the FT-IR spectra of *trans*-[RhX(=^{13}C=^{13}CH$_2$)(P*i*Pr$_3$)$_2$] (X = F, Cl, I).

ν(^{13}C=^{13}C) vibrational mode (Fig. 2). This band is red-shifted in the order F > Cl > I.

In the Raman spectra of the phenyl-substituted vinylidene complexes **5**–**10** (Fig. 3), the ν(Rh=C) mode was assigned to an absorption in the range of 567–579 cm^{-1} by analogy to *trans*-[RhF(=C=CH$_2$)(P*i*Pr$_3$)$_2$], for which the ν(Rh=C) mode was found at 572 cm^{-1}.[17] Additional support for this assignment arises from DFT calculations of the metal–carbon stretches for the model compounds *trans*-[RhX(=C=CHPh)(PMe$_3$)$_2$] (X = F, Cl, CH$_3$) using the DFT1 and 2 methods (Table 1). The order of the ν(Rh=C) wavenumbers for the phenyl-substituted vinylidene complexes **5**–**8** is F > Cl > Br > I (Fig. 3), which is similar to the order observed for **1**–**4**, although the differences between the wavenumbers are smaller. We attribute this result regarding the smaller differences in the position of the metal–carbon stretching band to a coupling between the ν(Rh=C) mode and an in-plane ring deformation mode,

Table 1 Calculated and experimental fundamental vibrational modes (cm^{-1}) in vinylidene rhodium complexes

Compound	Method	ν(C=C)	ν(Rh=C)	ν(Rh–X)
trans-[RhF(=C=CH$_2$)(P*i*Pr$_3$)$_2$][a]	IR	1628s	574m	458vs
	R	—	572vs	458m
trans-[RhF(=C=CH$_2$)(PMe$_3$)$_2$][a]	DFT1	1656	571	451
	DFT2	1655	570	433
	DFT3	1654	571	456
trans-[RhF(=C=CHPh)(P*i*Pr$_3$)$_2$] (**5**)	IR	1653m	577m	469s
	R	1653shm	579s	469shm
trans-[RhF(=C=CHPh)(PMe$_3$)$_2$]	DFT1	1652	582	456
	DFT2	1649	574	439
trans-[RhCl(=C=CHPh)(P*i*Pr$_3$)$_2$] (**6**)	IR	1649s	576s	—
	R	1640m	574s	281mw
trans-[RhCl(=C=CHPh)(PMe$_3$)$_2$]	DFT2	1652	570	301
trans-[RhCl(=C=CH$_2$)(PMe$_3$)$_2$]	DFT1	1659	563	282
trans-[RhBr(=C=CHPh)(P*i*Pr$_3$)$_2$] (**7**)	IR	1649s	575m	—
	R	1648m	573s	203m
trans-[RhBr(=C=CH$_2$)(PMe$_3$)$_2$]	DFT1	1659	558	205
trans-[RhI(=C=CHPh)(P*i*Pr$_3$)$_2$] (**8**)	IR	1638s	573s	—
	R	1639m	572s	150m?
trans-[RhI(=C=CH$_2$)(PMe$_3$)$_2$]	DFT1	1658	553	138
trans-[Rh(CH$_3$)(=C=CHPh)(P*i*Pr$_3$)$_2$] (**9**)	IR	1603, 1633m	571m	452wsh
	R	—	571m	452m
trans-[Rh(CH$_3$)(=C=CH$_2$)(PMe$_3$)$_2$]	DFT1	1601	528	463
trans-[Rh(CH$_3$)(=C=CHPh)(PMe$_3$)$_2$]	DFT1	1610	573	464
trans-[Rh(C≡CPh)(=C=CHPh)(P*i*Pr$_3$)$_2$] (**10**)	IR	1611, 1635m 1635vw	567m	—
	R		567s	540vs
trans-[Rh(C≡CPh)(=C=CHPh)(PMe$_3$)$_2$][b]	DFT1	1642	571	543

[a] Ref. 17. [b] ν(C≡C) 2072 cm^{-1}; calculated at 2062 cm^{-1} using DFT1.

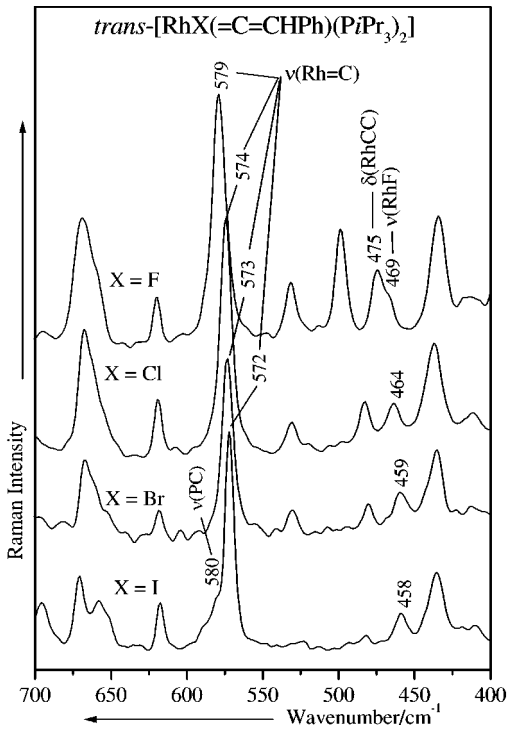

Fig. 3 The low-wavenumber region of the FT-Raman spectra of *trans*-[RhX(=C=CHPh)($P i Pr_3$)$_2$] (X = F, Cl, Br, I).

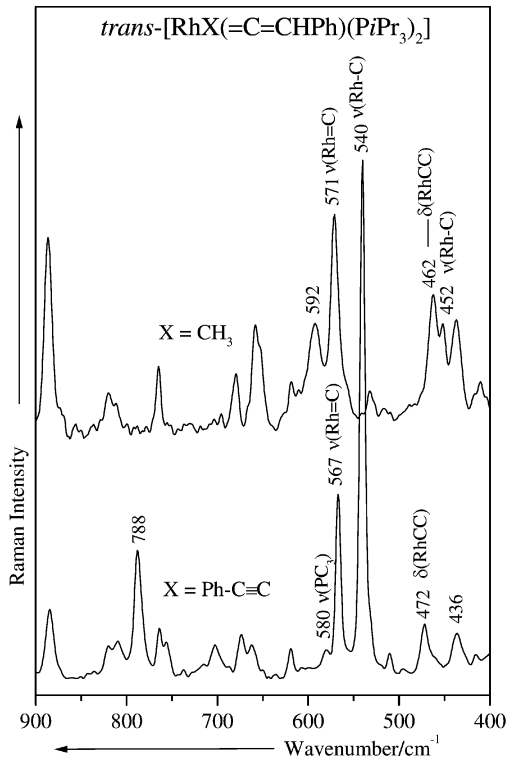

Fig. 4 The low-wavenumber region of the FT-Raman spectra of *trans*-[RhX(=C=CHPh)($P i Pr_3$)$_2$] (X = CH_3, C≡CPh).

which was confirmed by computer-animated vibrational simulation for the model compounds.

In addition to the ν(Rh=C) stretching vibration, two further modes are of great relevance for this study. First, the deformation mode δ(RhCC), which was observed in the FT-Raman spectra of the phenyl-substituted vinylidene complexes **5**–**8** (Fig. 3). This mode was predicted by the DFT2 method to be at 472 cm^{-1} for the model compound *trans*-[RhF(=C=CHPh)-(PMe_3)$_2$] and has been assigned to the band of medium intensity at 475 cm^{-1} in the FT-Raman spectrum of **5**. Second, the $C–C_{Ph}$ stretching mode for which a high Raman activity is characteristic. This mode was assigned on the basis of DFT calculations to the strong bands at 1230 (X = F; calc. 1231 cm^{-1}, DFT2), 1225 (X = Cl; calc. 1226 cm^{-1}, DFT2), 1224 (X = Br) and 1220 cm^{-1} (X = I) in the FT-Raman spectra of **5**–**8**. It is important to note that these modes have also been shifted to lower wavenumbers in the order F > Cl > Br > I, which again reflects the *trans* influence of the halide ligand in the rhodium(I) complexes.

The ν(C=C) modes were observed in the range between 1653 and 1603 cm^{-1} for compounds **5**–**10** and were active both in the Raman and infrared spectra. The corresponding order of X illustrating the *trans* influence is CH_3 > C≡CPh > I > Br, Cl > F.

The FT-Raman spectra of compounds **9** and **10** are more complicated in the low-wavenumber region (Fig. 4). Bands at 571 cm^{-1} for **9** and at 567 cm^{-1} for **10** were assigned to the ν(Rh=C) modes. This assignment agrees with the data found for complexes **5**–**8** and compares well with the calculated vibrational modes for the model compounds *trans*-[Rh(CH_3)(=C=CH_2)(PMe_3)$_2$], *trans*-[Rh(CH_3)(=C=CHPh)-(PMe_3)$_2$] and *trans*-[Rh(C≡CPh)(=C=CHPh)(PMe_3)$_2$] (Table 1). The positions of the ν(Rh–C) bands were temtatively located at 452 cm^{-1} for **9** and at 540 cm^{-1} for **10**, in agreement with the calculated values of 463 and 542 cm^{-1}, respectively.

The ν(C≡C) mode of compound **10** appeared as a strong band at 2072 cm^{-1} in the FT-Raman spectrum and as a medium band at 2071 cm^{-1} in the IR spectrum; it is red-shifted by 39 cm^{-1} compared with phenylacetylene (2111 cm^{-1}).[18] In the FT-Raman spectra of the analogous carbonyl complexes *trans*-[RhX(CO)($P i Pr_3$)$_2$] (X = F, Cl, Br, I), a band in the range between 573 and 546 cm^{-1} was assigned to the ν(Rh=C) mode (Fig. 5) on the basis of DFT calculations for the corresponding model compounds (Table 2). The position of this mode is dependent on the halide ligand, as observed for the rhodium–carbon stretching mode of the vinylidene complexes **1**–**10**. The ν(CO) mode was found at 1929–1943 cm^{-1}

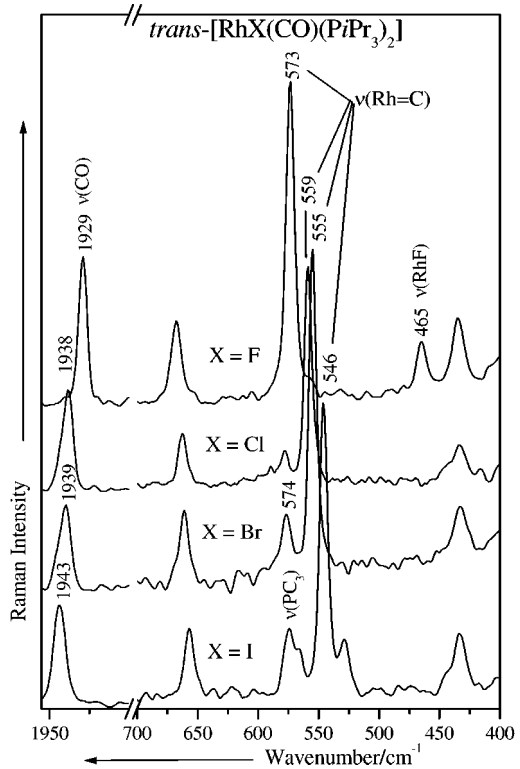

Fig. 5 The ν(CO) and ν(Rh=C) wavenumber region of the FT-Raman spectra of *trans*-[RhX(CO)($P i Pr_3$)$_2$] (X = F, Cl, Br, I).

Table 2 Calculated and experimental fundamental vibrational modes (cm^{-1}) in carbonyl rhodium complexes

Compound	Method	ν(Rh=C)	ν(Rh–X)	ν(CO)
trans-[RhF(CO)(P*i*Pr$_3$)$_2$][a] (**11**)	IR	573m	465s	1934vs
	R	573vs	465m	1929s
trans-[RhF(CO)(PMe$_3$)$_2$][a]	DFT1	570	450	1843
trans-[RhCl(CO)(P*i*Pr$_3$)$_2$] (**12**)	IR	559mw	—	1938s
	R	559vs	277w?	1938s
trans-[RhCl(CO)(PMe$_3$)$_2$]	R[b]	550	303	1965
	DFT1	561	285	1848
	DFT2	547	283	1958
	DFT3	542	287	1954
trans-[RhBr(CO)(P*i*Pr$_3$)$_2$] (**13**)	IR	555w	—	1941s
	R	555s	227m	1940s
trans-[RhBr(CO)(PMe$_3$)$_2$]	R[b]	552	195	1961
	DFT1	557	205	1847
	DFT4	542	214	1957
trans-[RhI(CO)(P*i*Pr$_3$)$_2$] (**14**)	IR	546w	—	1944s
	R	546s	137m?	1943s
trans-[RhI(CO)(PMe$_3$)$_2$]	DFT1	551	139	1847
	DFT4	536	147	1957

[a] Ref. 17. [b] Ref. 41.

and its wavenumber decreases in the order I > Br > Cl > F (Fig. 5).

Since it is well known that δ(MCO) modes of metal carbonyl complexes give rise to intense bands at higher wavenumbers than those caused by metal–carbon stretching vibrations,[19] the strong band at 601 cm^{-1} in the FT-Raman spectrum of the fluoro complex **11** can probably be assigned to the δ(RhCO) mode. In the spectra of the chloro, bromo and iodo carbonyl compounds, the corresponding band for the δ(RhCO) mode is shifted to lower wavenumbers and found at 582, 576 and 566 cm^{-1}, respectively (Fig. 6). In the structurally related compounds *trans*-[RhX(CO)(PPh$_3$)$_2$], the δ(RhCO) deformation mode has been assigned at 596, 574, 567 and 558 cm^{-1} for X = F, Cl, Br and I, respectively,[20] which is in good agreement with our results.

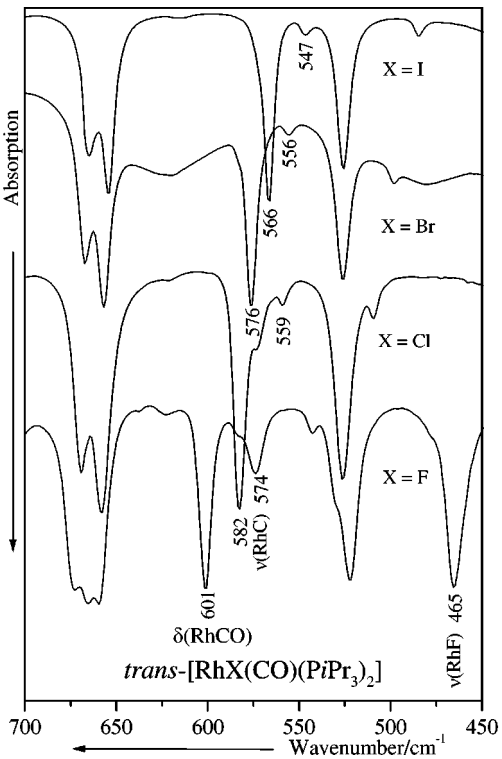

Fig. 6 The δ(RhCO) and ν(Rh=C) wavenumber region of the FT-IR spectrum of *trans*-[RhX(CO)(P*i*Pr$_3$)$_2$] (X = F, Cl, Br, I).

DFT calculations

DFT calculations have been carried out for the model compounds *trans*-[RhX(L)(PMe$_3$)$_2$] (L = C=CH$_2$ and CO; X = F, Cl, Br, I and CH$_3$) and *trans*-[RhX(=C=CHPh)(PMe$_3$)$_2$] (X = F, Cl, CH$_3$ and C≡CPh). The isopropyl groups of the experimental complexes have been substituted by methyl groups in order to reduce the computation time. As expected, the BPW91 DFT method with the Los Alamos pseudopotential plus double zeta (LANL2DZ) for rhodium in combination with the Dunning/Huzinaga full double zeta (D95) or the Pople basis sets in combination with polarization and diffuse functions gave the best results for the series of the vinylidene halide and the carbonyl halide complexes. The agreement between the calculated and the experimental bond distances and bond angles for analogous compounds was quite good (see Tables 3 and 4).

The addition of polarization and diffuse functions to the small basis set LANL2DZ provides in general better structural parameters, particularly for the Rh–P bond lengths and improves significantly the resulting ν(CO) vibrational modes (Tables 2–4). It should be noted that the good agreement of the BPW91/LANL2DZ vibrational modes with the experimental data is most likely due to favorable error cancellation. The calculated structure of *trans*-[Rh(C≡CPh)(=C=CHPh)(PMe$_3$)$_2$] with the small basis LANL2DZ was acceptable but for *trans*-[Rh(CH$_3$)(=C=CHR)(PMe$_3$)$_2$] (R = H or Ph) the calculated C–Rh–C and Rh–C–C bond angles were too small (157.2 and 158.6°) for the minimum energy structure. The freezing of both the C–Rh–C and Rh–C–C bond angles to 180° leads to a linear structural arrangement with one imaginary harmonic wavenumber corresponding to a C–Rh–C–C bending mode indicating a saddle point. The energy difference between the two structures was less than 6 kJ mol^{-1}.

For the calculation of atomic charges, natural bond orbital (NBO) calculations were performed for the model compounds *trans*-[RhX(=C=CH$_2$)(PMe$_3$)$_2$] (X = F, Cl, Br, I and CH$_3$) and *trans*-[RhX(CO)(PMe$_3$)$_2$] (X = F, Cl, Br, I). The resulting natural population analysis (NPA)[21] gave the partial charges represented in Tables 5 and 6.

The energies of the molecular orbitals for the model compounds *trans*-[RhX(L)(PMe$_3$)$_2$] (L = C=CH$_2$, X = F, Cl, Br, I and CH$_3$; L = CO, X = F, Cl, Br, I) were calculated by using DFT1 and DFT4 (see Table 7). The geometries of the LUMO and HOMO of the vinylidene (X = F, CH$_3$) and carbonyl compounds (X = F) are depicted in Fig. 7. The LUMO of the vinylidene complex is a combination of the p$_z$(F), d$_{xz}$(Rh) and

Table 3 Selected bond lengths (pm) and angles (°) calculated for the model compounds *trans*-[RhX(=C=CHR)(PMe_3)$_2$], together with the experimental values found in *trans*-[RhCl(=C=CHMe)($PiPr_3$)$_2$]

Compound	Rh–X	Rh=C	C=C	Rh–P	P–Rh–X	P–Rh–C	X–Rh–C	Method
trans-[RhF(=C=CH_2)(PMe_3)$_2$]	205.5	182.0	134.1	238.5	84.6	95.4	179.4	DFT1
trans-[RhF(=C=CHPh)(PMe_3)$_2$]	205.2	181.3	135.1	239.0	84.5	95.5	178.8	DFT1
trans-[RhCl(=C=CH_2)(PMe_3)$_2$]	247.3	182.3	134.0	239.7	86.9	93.1	179.4	DFT1
	242.1	181.4	132.5	232.9	87.5	92.5	179.8	DFT3
	244.2	181.7	132.7	234.9	87.3	92.7	179.9	DFT4
trans-[RhCl(=C=CHPh)(PMe_3)$_2$]	243.9	181.1	134.1	236.0	87.6	92.4	179.7	DFT2
trans-[RhBr(=C=CH_2)(PMe_3)$_2$]	261.8	182.6	133.9	240.0	87.7	92.3	180.0	DFT1
trans-[RhI(=C=CH_2)(PMe_3)$_2$]	278.5	182.9	133.9	240.6	88.7	91.3	180.0	DFT1
trans-[Rh(CH_3)(=C=CH_2)(PMe_3)$_2$]	214.0	187.7	134.9	238.0	89.3	90.8	157.2	DFT1
	214.8	186.7	133.4	232.6	89.1	90.9	155.8	DFT4
trans-[Rh(CH_3)(=C=CHPh)(PMe_3)$_2$]	213.6	187.1	136.0	238.6	89.2	90.9	154.8	DFT1
trans-[Rh(C≡CPh)(=C=CHPh)(PMe_3)$_2$]	203.5	186.4	135.0	239.3	87.3	92.7	171.4	DFT1
trans-[RhCl(=C=CHMe)($PiPr_3$)$_2$]	236.6(2)	177.5(6)	132.0(1)	234.4(2)	91.95(7)	88.2(2)	175.8(2)	X-Ray[a]
				234.2(2)	91.19(7)	89.1(2)		

[a] Ref. 42.

Table 4 Selected bond lengths (pm) and angles (°) calculated for the model compounds *trans*-[RhX(CO)(PMe_3)$_2$], together with the experimental values found in *trans*-[RhF(CO)(PPh_3)$_2$] and *trans*-[RhCl(CO)(PMe_3)$_2$]

Compound	Rh–X	Rh=C	C–O	Rh–P	P–Rh–X	P–Rh–C	X–Rh–C	Method
trans-[RhF(CO)(PMe_3)$_2$]	205.2	181.7	120.9	238.5	82.7	97.3	179.8	DFT1
	204.4	181.1	117.6	231.9	84.1	95.9	179.7	DFT3
trans-[RhCl(CO)(PMe_3)$_2$]	246.5	182.0	120.7	239.6	85.6	94.4	180.0	DFT1
	241.2	182.0	117.3	232.6	86.4	93.6	180.0	DFT3
trans-[RhBr(CO)(PMe_3)$_2$]	260.7	182.2	120.7	240.0	86.6	93.4	180.0	DFT1
	256.0	182.7	117.8	235.0	87.0	93.0	180.0	DFT4
trans-[RhI(CO)(PMe_3)$_2$]	277.1	182.6	120.6	240.6	87.7	92.3	180.0	DFT1
	274.4	183.1	117.8	235.1	87.8	92.2	180.0	DFT4
trans-[RhF(CO)(PPh_3)$_2$]	204.6(2)	179.6(3)	115.1(4)	233.0(7)	86.9(5)	91.3(5)		X-Ray[a]
				232.4(7)	88.1(9)	93.7(9)		
trans-[RhCl(CO)(PMe_3)$_2$]	235.4(1)	177.0(4)	114.6(4)	230.9(1)	88.1(0)	91.6(1)	179.4(1)	X-Ray[b]
				230.7(1)	89.3(0)	91.0(1)		

[a] Ref. 43. [b] Ref. 44.

$p_z(C_2)$ orbitals, the contribution of the p_z(β-C) orbital being the most important. For the carbonyl complex, the LUMO is a combination of p_z(CO) and Rh π-orbitals. The HOMO is mainly composed of the d_{z^2} orbital of Rh in both complexes.

Table 5 Partial charges *q* on selected atoms of the model complexes *trans*-[RhX(=C=CH_2)(PMe_3)$_2$] determined by natural population analysis

X =	X	Rh	C_α	C_β	Method
F	−0.65	+0.03	+0.04	−0.68	DFT1
	−0.71	+0.01	+0.11	−0.75	DFT4
Cl	−0.59	−0.07	+0.05	−0.66	DFT1
	−0.61	−0.10	+0.12	−0.74	DFT4
Br	−0.57	−0.09	+0.05	−0.66	DFT1
	−0.55	−0.15	+0.11	−0.74	DFT4
I	−0.54	−0.11	+0.04	−0.66	DFT1
	−0.49	−0.15	+0.11	−0.74	DFT4
CH_3	−1.02[a]	−0.06	−0.07	−0.67	DFT1
	−1.03[a]	−0.09	+0.005	−0.75	DFT4

[a] Charge on the carbon atom of the methyl group.

Table 6 Partial charges *q* on selected atoms of the model complexes *trans*-[RhX(CO)(PMe_3)$_2$] determined by natural population analysis[a]

X =	X	Rh	C	O
F	−0.64	−0.05	+0.42	−0.50
Cl	−0.58	−0.19	+0.45	−0.49
Br	−0.56	−0.21	+0.45	−0.48
I	−0.52	−0.23	+0.44	−0.48

[a] BPW91/LANL2DZ was used for all atoms (DFT1).

The shapes of the HOMO and LUMO do not change along the series of compounds involved in the calculations with the exception of the methyl vinylidene complex (see Fig. 7). Similar atomic orbital combinations for the LUMO and HOMO were obtained by Cauletti and coworkers for *trans*-[RhCl(=C=CH_2)(PMe_3)$_2$] using DV-Xα calculations.[22] However, the calculated MO energies using the DFT1–4 methods (Table 7) are about 1 eV smaller than those using DV-Xα. The reason for this difference could be due to the fact that the DV-Xα calculations were performed without a correlation functional in contrast to the exchange and gradient-corrected correlation functional (BPW91) used in this study (see computational details). The calculated energies with the DFT1 method were higher than those calculated using the DFT2–4 methods, which gave very similar results. However, for the vinylidene complexes the resulting difference $\Delta E_{LUMO-HOMO}$ is nearly independent of the method used. For the carbonyl compounds, the calculated differences between the LUMO and the HOMO using DFT1 were 0.2–0.3 eV smaller than those calculated with the DFT2–4 methods. The calculated orbital energies for the phenyl-substituted vinylidenes *trans*-[RhX(=C=CHPh)(PMe_3)$_2$] were lower than in the related complexes containing the C=CH_2 ligand.

The calculated difference $\Delta E_{LUMO-HOMO}$ for the model compounds *trans*-[RhX(=C=CH_2)(PMe_3)$_2$] is in fair agreement with the energies of the lowest energy absorption E_{max} of **1**–**10** in the visible region and also decreases in the order F > Cl ⩾ Br > I for **1**–**4**, and F > CH_3 > Cl ≈ Br > I > C≡CPh for **5**–**10** (Table 7). For the methyl complex, the LANL2DZ method gave a value of $\Delta E_{LUMO-HOMO}$ in the minimum energy structure that also agrees with the spectroscopic data, despite the unusual C–Rh–C bond angle of

Table 7 Energies of the molecular orbitals, orbital energy differences and energies of the lowest energy visible absorption maxima (all in eV) for vinylidene and carbonyl rhodium complexes

Compound	Method	E_{LUMO}	E_{HOMO}	$\Delta E_{LUMO-HOMO}$	E_{max} (Compound)[a]
trans-[RhF(=C=CH_2)(PMe_3)$_2$]	DFT1	−1.99	−4.15	2.16	2.37 (**1**)
	DFT2	−2.23	−4.39	2.16	
	DFT3	−2.21	−4.40	2.19	
	DFT4	−2.25	−4.41	2.16	
trans-[RhF(=C=CHPh)(PMe_3)$_2$]	DFT1	−2.24	−4.26	2.02	2.25 (**5**)
trans-[RhCl(=C=CH_2)(PMe_3)$_2$]	DFT1	−2.32	−4.35	2.03	2.20 (**2**)
					2.12 (**6**)
trans-[RhBr(=C=CH_2)(PMe_3)$_2$]	DFT1	−2.41	−4.40	1.99	2.16 (**3**)
					2.13 (**7**)
trans-[RhI(=C=CH_2)(PMe_3)$_2$]	DFT1	−2.47	−4.41	1.94	2.12 (**4**)
					2.06 (**8**)
trans-[Rh(CH_3)(=C=CH_2)(PMe_3)$_2$]	DFT1	−1.62	−3.77	2.15	
trans-[Rh(CH_3)(=C=CHPh)(PMe_3)$_2$]	DFT1	−1.82	−3.98	2.16	2.22 (**9**)
trans-[Rh(C≡CPh)(=C=CHPh)(PMe_3)$_2$]	DFT1	−2.51	−4.29	1.78	2.03 (**10**)
trans-[RhF(CO)(PMe_3)$_2$]	DFT1	−1.24	−4.11	2.87	3.53 (**11**)
trans-[RhCl(CO)(PMe_3)$_2$]	DFT1	−1.55	−4.33	2.78	3.43 (**12**)
trans-[RhBr(CO)(PMe_3)$_2$]	DFT1	−1.65	−4.38	2.73	3.41 (**13**)
trans-[RhI(CO)(PMe_3)$_2$]	DFT1	−1.73	−4.42	2.69	3.35 (**14**)

[a] In hexane.

157.2°. In contrast, the linear structure gives a $\Delta E_{LUMO-HOMO}$ of 1.81 eV (DFT1), which differs from the observed trend of the energies of the absorption maxima in the visible region. For the carbonyl compounds, the calculated energy differences between LUMO and HOMO and the energies of the observed absorption maxima both follow the same trend as in the vinylidene complexes, although the difference between the calculated and the experimental energies is larger.

Since the HOMO is mainly located on Rh and the LUMO mainly on the vinylidene or partially on the carbonyl ligand, the corresponding absorptions could be classified as metal-to-ligand charge transfer bands. Also, the absorptions in the visible spectra of the related compounds *trans*-[RhX(CY)(PR_3)$_2$] (Y = O,[23] Y = S[24]) have been attributed to MLCT transitions.

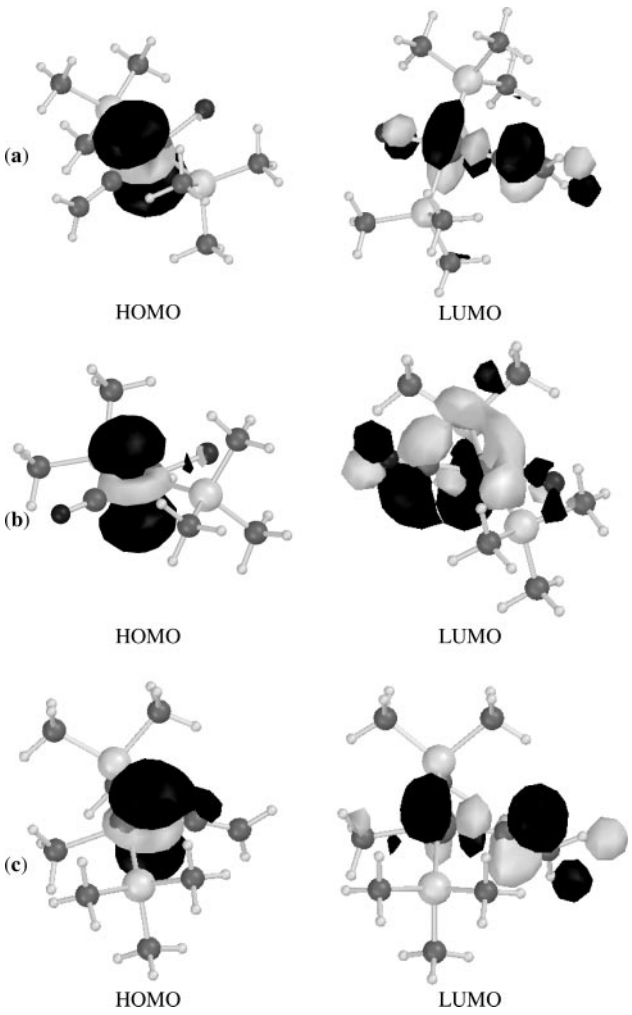

Fig. 7 Representation of the calculated LUMOs and HOMOs (0.04 a.u.) of (a) *trans*-[RhF(=C=CH_2)(PMe_3)$_2$], (b) *trans*-[RhF(CO)(PMe_3)$_2$] and (c) *trans*-[Rh(CH_3)(=C=CH_2)(PMe_3)$_2$].

Discussion

For a diatomic molecule, the vibrational mode is directly related to $(k/m)^{1/2}$, where k is the force constant of the bond and m is the reduced mass. Since the force constant reflects the bond strength, the conclusion is that the stronger the bond, the higher its wavenumber. In polyatomic molecules, the same principle has been generally applied to bands that mainly originate from the stretching of one particular bond.

Recently, we have studied the vibrational spectra of the square-planar vinylidene complexes *trans*-[RhF(=C=CH_2)($PiPr_3$)$_2$] and its ^{13}C-containing isotopomer *trans*-[RhF(=^{13}C=$^{13}CH_2$)($PiPr_3$)$_2$] (**1**) and found that, by using FT-Raman spectroscopy, the ν(Rh=C) and ν(Rh=^{13}C) modes can be unambiguously assigned.[17] In the ^{13}C-substituted compounds, the ν(Rh=^{13}C) mode gives rise to an intense band that is separated from the others, while in *trans*-[RhX(=C=CH_2)($PiPr_3$)$_2$] a band of medium-to-weak intensity, originating from the phosphines, overlaps with the ν(Rh=C) mode. Due to these observations, the series of ^{13}C-labeled complexes *trans*-[RhX(=^{13}C=$^{13}CH_2$)($PiPr_3$)$_2$] (**1**–**4**) is an appropriate system to study the variation of ν(Rh=^{13}C) as a probe of the electronic influence of the ligand X *trans*-disposed to the Rh=C bond. This investigation has been extended to the phenyl-substituted vinylidene complexes **5**–**10** and to the related carbonyl derivatives **11**–**14**.

From the data of the Raman spectra of the vinylidene compounds **1**–**10** (Fig. 1 and Table 1), for different ligands X the following order of the ν(Rh=^{13}C) and ν(Rh=C) wavenumbers has been obtained: F > Cl ≥ Br ≥ I > CH_3 > C≡CPh. We have already mentioned that the coupling between the ν(Rh=C) and ν(RhX) modes as well as the mass effect of the heavier halogens also contribute to this sequence. However, the fact that the calculated Rh=C distances for the model compounds *trans*-[RhX(=C=CH_2)(PMe_3)$_2$] increase in the same

order as the wavenumber of the ν(Rh=C) modes decreases suggests that the observed sequence is mainly due to a variation in the Rh=C bond strengths.

Since for the series of halide complexes, the order of the ν(Rh=C) stretching mode is the same for **1**–**4** as for **5**–**8**, we assume that the bonding properties of the C=CH_2 and C=CHPh ligands are quite similar. A slightly exceptional observation is that the wavenumber of the ν(Rh=C) mode for compound **5** is 7 cm^{-1} higher in the Raman spectrum than for *trans*-[RhF(=C=CH_2)(P*i*Pr_3)$_2$]. Although this increase might indicate that substitution of H by Ph strengthens the Rh=C bond, it could also originate from the above-mentioned coupling between the ν(Rh=C) and an in-plane ring deformation mode. By taking this into consideration, we conclude that on the basis of the vibrational spectra the *trans* influence of the ligands X in compounds **1**–**10** decreases along the series C≡CPh > CH_3 > I > Br > Cl > F.

It is interesting to compare the variations of the vibrational data of the vinylidene compounds **1**–**4** with those of the isoelectronic carbonyls *trans*-[RhX(CO)(P*i*Pr_3)$_2$], where X = F (**11**), Cl (**12**), Br (**13**) and I (**14**). In the FT-Raman spectra of **11**–**14**, the ν(Rh=C) mode is shifted to lower wavenumbers in the order F > Cl > Br > I (Fig. 5), which is the same as found for the analogous vinylidene complexes **1**–**4** (Fig. 1). However, while the ν(CO) mode of **11**–**14** is shifted to higher wavenumbers along the sequence F < Cl < Br < I (Fig. 6), the ν(^{13}C=^{13}C) and ν(C=C) modes of **1**–**4** (Fig. 2) and **5**–**8** (Table 1) are shifted to higher wavenumbers in the opposite sequence. The observed opposite trends of ν(CO) and δ(RhCO) for **11**–**14** (Fig. 5 and 6) is the same as that observed for the triphenylphosphine complexes *trans*-[RhX(CO)(PPh_3)$_2$] (X = F, Cl, Br, I),[20,25] and has been explained in terms of an increasing π-donor capability of X on going up in group 17. The surprising situation thus arises that the metal center seems to be more electron-rich if it is bonded to a more electronegative halogen. This supposition has been used to explain the variation of the half-wave reduction potentials and the equilibrium constants for the halide exchange in *trans*-[RhX(CO)(PPh_3)$_2$] (X = F, Cl, Br, I)[20,25] as well as in related halide complexes of Fe,[2] Ru,[26] Ir[3] and Pd.[27] With regard to our work, the same clue about a push-pull π-interaction, X → Rh → C, provides an explanation for why we find for both the vinylidene and the carbonyl complexes the highest Rh–C bond strength when fluoride is the *trans*-disposed ligand.

Quite remarkably, the calculated atomic charges for the model compounds *trans*-[RhX(L)(PMe_3)$_2$], where L = C=CH_2 or CO and X = F, Cl, Br, I and CH_3, are not in agreement with the assumption that the metal center becomes more electron-rich along the sequence F > Cl > Br > I > CH_3 (see Tables 5 and 6). According to the calculations, the positive charge on Rh increases from X = I to X = F while the charge on the vinylidene and CO ligands does not vary significantly. In addition, the calculated population of the p_π orbitals of the halogens does not vary significantly in the series, suggesting that the shifts of the vibrational modes are not caused by differences in p_π donation from the halogen to the metal. In the case of the fluoro complexes, the considerable difference in charge between Rh and F (0.68 for L = C=CH_2 and 0.59 for L = CO), calculated by the DFT1 method, suggests that (i) the Rh–F bond has a strong electrostatic component and (ii) the small and highly negatively charged fluorine atom will cause severe electrostatic repulsions with the electron density at the metal.[28] Thus, the coordination of fluoride has two effects on the Rh–C bond. On the one hand, the higher positive charge on the metal leads to an increase in the σ-donation from carbon to rhodium, while on the other hand the repulsion between the p_π electrons of the fluoride and the d_π electrons of rhodium favors a π-retrodonation from the metal to the empty p_π orbitals of the vinylidene ligand. In addition to these two effects, the electrostatic behavior of rhodium may also play a role in the observed variation of the ν(CO) mode, since it has been shown that the electrostatic influence of a positively charged atom bonded to CO initiates a shift of the CO stretching vibration to lower wavenumbers.[29]

The discussed repulsion between filled orbitals can also be used to explain the variation of the calculated energies of the HOMOs for the model compounds *trans*-[RhX(=C=CH_2)(PMe_3)$_2$] where X = F, Cl, Br and I (Table 7). The energy of the HOMO decreases along the sequence F > Cl > Br > I, the difference between the fluoro and the chloro complex being the highest. This result agrees with the fact that fluorine, as the group 17 element with the smallest radius and the largest negative charge, creates the strongest destabilizing repulsion with the electrons of the HOMO, which is mainly composed of the d_{z^2} orbital of Rh. Regarding the LUMOs, their energy also decreases along the sequence F > Cl > Br > I (see Table 7). A possible explanation for this trend could be that due to the Rh=C antibonding character of the LUMOs (see Fig. 7) these orbitals will be higher in energy if the strength of the Rh=C bond increases. With respect to the analogous model compounds containing CO instead of C=CH_2, the HOMOs are strongly localized on the metal and include only some minor contributions from the CO carbon atom. Although the calculated energies of the HOMOs for the carbonyl and the vinylidene complexes are quite similar (see Table 7), the energies of the LUMOs are somewhat higher for L = CO than for L = C=CH_2. This difference causes the observed blue-shift of the absorption maxima in the visible region.

An interesting situation results for the model compound *trans*-[Rh(CH_3)(=C=CH_2)(PMe_3)$_2$], in which the methyl ligand has no nonbonding electrons that could initiate a repulsion with the d electrons of rhodium. The minimum energy structure calculated by the BPW91/LANL2DZ method for *trans*-[Rh(CH_3)(=C=CH_2)(PMe_3)$_2$] reveals a significant distortion from the anticipated linear C–Rh=C=C chain, the calculated C–Rh–C and Rh–C–C bond angles being 157.2 and 158.6°, respectively. However, the energy of the distorted structure for the vinylidene complex is less than 6 kJ mol^{-1} smaller than the energy for the linear arrangement. In this context, it should be noted that in benzene compound **9** rearranges to the π-allyl complex [Rh(η^3-CH_2CH-CHPh)(P*i*Pr_3)$_2$] by migration of the methyl group to the vinylidene ligand.[30] Therefore, a coupling of the two C-bonded ligands is possible, even without the presence of a supporting Lewis base. Although in this case we should be more cautious regarding the calculated Rh=C bond distance and the value of the assigned ν(Rh=C) mode, the calculation suggests that the Rh=C bond is weaker. This can be rationalized by assuming that the electrostatic repulsion, which in the halide complexes pushes the d_π orbitals towards the p_π orbitals of the carbon, is not present in the methyl compound. The calculated charge of the metal in the methyl rhodium complex lies between that of the fluoro and the chloro derivatives.

Conclusions

The values of the Rh=C stretching mode for the vinylidene complexes *trans*-[RhX(=C=CHR)(P*i*Pr_3)$_2$], where R = H or Ph, suggest that the strength of the Rh=C bond increases along the sequence X = C≡CPh < CH_3 < I < Br < Cl < F. The calculated Rh=C bond distances for the model compounds *trans*-[RhX(=C=CH_2)(PMe_3)$_2$] decrease in the same sequence. The NPA analysis reveals that the metal becomes more electron-rich by varying the ligand X along the sequence F < CH_3 < Cl < Br < I. These results can be explained by taking two effects into consideration. First, with the increase of the electronegativity of X the charge of the metal becomes more positive and the σ-donation from carbon to rhodium

becomes stronger. Second, with the increase of the charge on X accompanied by a decrease in size the repulsion between the nonbonding electron pairs of X and the filled d_π orbitals of Rh become stronger. The latter effect leads to an increase in π-backbonding from the metal to the empty p_π orbital of carbon. For the series of carbonyl compounds *trans*-[RhX(CO)(P*i*Pr$_3$)$_2$], where X = F, Cl, Br and I, analogous results have been obtained and confirmed for the model compounds *trans*-[RhX(CO)(PMe$_3$)$_2$].

Experimental

All reactions were carried out under an inert atmosphere of argon by use of Schlenk techniques. Compounds **1**,[17] **5**,[31] **6**,[32] **9**,[33] **10**,[34] **11**[31] and **12**[35] were prepared as reported previously. NMR spectra were recorded at room temperature on Bruker AC 200 and Bruker AMX 400 instruments [abbreviations used: s, singlet; d, doublet; t, triplet; m, multiplet; vt, virtual triplet; br, broadened signal; coupling constants *N* and *J* in Hz]. The FT-Raman spectra were recorded at room temperature using a Bruker IFS 120-HR spectrometer with an integrated FRA 106 Raman module (resolution = 3 cm^{-1}). Radiation of 1064 nm from a Nd-YAG laser was employed for excitation of crystalline samples contained in NMR tubes under argon. The infrared spectra were recorded with a Bruker IFS 25 spectrometer using Nujol suspensions between KBr plates. UV-visible spectra were recorded using *n*-hexane solutions in the range 300–700 nm using a Perkin–Elmer UV/VIS/NIR Lambda 19 spectrometer with the wavelength of the lamp at 319.2 and 860.8 nm and filters at 810.4, 690.4, 562.4 and 379.2 nm. The detector used for the UV/VIS region was a photomultiplier.

Syntheses

***trans*-[RhCl(=^{13}C=^{13}CH$_2$)(P*i*Pr$_3$)$_2$], 2.** A solution of **1** (230 mg, 0.49 mmol) in acetone (10 cm^3) was treated with KCl (73 mg, 0.98 mol) at room temperature. The suspension was stirred for 7 h and brought to dryness *in vacuo*. The residue was extracted twice with 10 cm^3 portions of pentane. The extract was filtered, concentrated to *ca.* 2 cm^3 and then stored for 24 h at −78 °C. Dark violet crystals precipitated, which were washed twice with 2 cm^3 portions of pentane (−35 °C) and dried *in vacuo*: yield 146 mg (62%). NMR (C_6D_6) δ_H (200 MHz) 2.84 (6 H, m, PC*H*CH$_3$), 1.30 [36 H, dvt, *N* 13.4, *J*(H,H) 7.3, PCHC*H*$_3$], −0.15 [2 H, ddt, *J*(P,H) 3.7, ^2J(C,H) 7.3, ^1J(C,H) 162.2, Rh=C=CH]; δ_C (50.3 MHz) 290.6 [ddt, *J*(C,C) 113.2, *J*(Rh,C) 56.6, *J*(P,C) 15.9, Rh=C], 89.1 [ddt, *J*(C,C) 56.0, *J*(Rh,C) 16.5, *J*(P,C) 5.5, Rh=C=*C*], 23.4 (vt, *N* 9.2, P*C*HCH$_3$), 20.2 (s, PCH*C*H$_3$); δ_P (81.0 MHz) 42.4 [ddd, *J*(Rh,P) 134.9, ^2J(C,P) 15.4, ^3J(C,P) 5.0].

***trans*-[RhBr(=^{13}C=^{13}CH$_2$)(P*i*Pr$_3$)$_2$], 3.** This compound was prepared analogously as described for **2**, using **1** (150 mg, 0.32 mmol) and KBr (55 mg, 0.46 mmol) as starting materials. Dark violet crystals: yield 126 mg (77%). NMR (C_6D_6) δ_H (400 MHz) 2.92 (6 H, m, PC*H*CH$_3$), 1.29 [36 H, dvt, *N* 13.8, *J*(H,H) 7.1, PCHC*H*$_3$], −0.44 [2 H, ddt, *J*(P,H) 3.4, ^2J(C,H) 6.7, ^1J(C,H) 161.7, Rh=C=CH]; δ_C (100.6 MHz) 287.8 [ddt, *J*(C,C) 115.3, *J*(Rh,C) 58.6, *J*(P,C) 16.2, Rh=C], 89.3 [ddt, *J*(C,C) 56.6, *J*(Rh,C) 17.2, *J*(P,C) 6.1, Rh=C=*C*], 23.8 (vt, *N* 10.1, P*C*HCH$_3$), 20.2 (s, PCH*C*H$_3$); δ_P (162.0 MHz) 40.9 [ddd, *J*(Rh,P) 133.9, ^2J(C,P) 15.3, ^3J(C,P) 5.1].

***trans*-[RhI(=^{13}C=^{13}CH$_2$)(P*i*Pr$_3$)$_2$], 4.** This compound was prepared analogously as described for **2**, using **1** (126 mg, 0.27 mmol) and NaI (53 mg, 0.35 mmol) as starting materials. Dark violet crystals: yield 110 mg (80%). NMR (C_6D_6) δ_H (400 MHz) 3.03 (6 H, m, PC*H*CH$_3$), 1.29 [36 H, dvt, *N* 13.3, *J*(H,H) 6.9, PCHC*H*$_3$], −0.64 [2 H, ddt, *J*(P,H) 3.4, ^2J(C,H) 6.9, ^1J(C,H) 161.9, Rh=C=CH]; δ_C (100.6 MHz) 283.4 [ddt, *J*(C,C) 116.3, *J*(Rh,C) 60.7, *J*(P,C) 16.2, Rh=C], 90.0 [ddt, *J*(C,C) 55.6, *J*(Rh,C) 16.2, *J*(P,C) 6.1, Rh=C=*C*], 25.0 (vt, *N* 10.1, P*C*HCH$_3$), 20.3 (s, PCH*C*H$_3$); δ_P (162.0 MHz) 40.2 [ddd, *J*(Rh,P) 132.2, ^2J(C,P) 15.3, ^3J(C,P) 6.8].

***trans*-[RhBr(=C=CHPh)(P*i*Pr$_3$)$_2$], 7.** A solution of **6** (175 mg, 0.31 mmol) in acetone (10 cm^3) was treated with KBr (500 mg, 4.2 mmol). The suspension was stirred at room temperature for 40 min and brought to dryness *in vacuo*. The residue was extracted twice with 12 cm^3 portions of hexane. The extract was filtered, concentrated to *ca.* 3 cm^3 and then stored for 2 days at −65 °C. Dark blue crystals precipitated, which were washed three times with 4 cm^3 portions of pentane (−40 °C) and dried *in vacuo*: yield 110 mg (59%). Anal. found: C, 51.72; H, 7.98%. $C_{26}H_{48}BrP_2Rh$ requires: C, 51.58; H, 7.99%. NMR (C_6D_6) δ_H (400 MHz) 7.16 (2 H, m, *ortho*-H of C_6H_5), 7.01 (2 H, m, *meta*-H of C_6H_5), 6.86 (1 H, m, *para*-H of C_6H_5), 2.80 (6 H, m, PC*H*CH$_3$), 1.28 [36 H, dvt, *N* 13.5, *J*(H,H) 6.4, PCHC*H*$_3$], 1.13 [1 H, t, *J*(P,H) 3.2, Rh=C=CH]; δ_C (100.6 MHz) 292.0 [dt, *J*(Rh,C) 59.8, *J*(P,C) 15.9, Rh=C], 128.6, 125.9, 125.2, 124.7 (all s, C_6H_5), 112.5 [dt, *J*(Rh,C) 15.3, *J*(P,C) 6.4, Rh=C=*C*H], 24.5 (vt, *N* 20.4, P*C*HCH$_3$), 20.4 (s, PCH*C*H$_3$); δ_P (81.0 MHz) 41.9 [d, *J*(Rh,P) 133.4].

***trans*-[RhI(=C=CHPh)(P*i*Pr$_3$)$_2$], 8.** This compound was prepared analogously as described for **7**, using **6** (257 mg, 0.46 mmol) and NaI (2.0 g, 13.3 mmol) as starting materials. Blue-green crystals: yield 210 mg (70%). Anal. found: C, 47.95; H, 7.31%. $C_{26}H_{48}IP_2Rh$ requires: C, 47.87; H, 7.42%. NMR (C_6D_6) δ_H (400 MHz) 7.14 (2 H, m, *ortho*-H of C_6H_5), 7.08 (2 H, m, *meta*-H of C_6H_5), 6.85 (1 H, m, *para*-H of C_6H_5), 2.89 (6 H, m, PC*H*CH$_3$), 1.27 [36 H, dvt, *N* 13.8, *J*(H,H) 6.7, PCHC*H*$_3$], 0.75 [1 H, t, *J*(P,H) 3.4 Hz, Rh=C=CH]; δ_C (100.6 MHz) 286.9 [dt, *J*(Rh,C) 63.6, *J*(P,C) 15.9, Rh=C], 128.6, 126.1, 125.4, 123.6 (all s, C_6H_5), 113.0 [dt, *J*(Rh,C) 15.3, *J*(P,C) 6.4, Rh=C=*C*H], 25.7 (vt, *N* 21.6, P*C*HCH$_3$), 20.6 (s, PCH*C*H$_3$); δ_P (81.0 MHz) 41.4 [d, *J*(Rh,P) 132.2].

***trans*-[RhBr(CO)(P*i*Pr$_3$)$_2$], 13.** A solution of **12** (201 mg, 0.41 mmol) in acetone (15 cm^3) was treated with NaBr (255 mg, 0.17 mol) at room temperature. The suspension was stirred for 60 h and brought to dryness *in vacuo*. The residue was extracted twice with 10 cm^3 portions of C_6H_6. The extract was filtered and the solvent was evaporated *in vacuo*. The residue was dissolved in 3 cm^3 of pentane and the solution stored for 18 h at −78 °C. Yellow crystals precipitated, which were washed twice with 3 cm^3 portions of pentane (−30 °C) and dried *in vacuo*: yield 210 mg (96%); mp 154 °C (decomp.). Anal. found: C, 42.96; H, 7.70%. $C_{19}H_{42}BrOP_2Rh$ requires: C, 42.95; H, 7.97%. NMR (CD_2Cl_2) δ_H (400 MHz) 2.70 (6 H, m, PC*H*CH$_3$), 1.30 [36 H, dvt, *N* 13.8, *J*(H,H) 6.8, PCHC*H*$_3$]; δ_C (100.6 MHz) 188.5 [dt, *J*(Rh,C) 75.8, *J*(P,C) 14.2, CO], 25.3 (vt, *N* 11.1, P*C*HCH$_3$), 20.3 (s, PCH*C*H$_3$); δ_P (162.0 MHz) 47.7 [d, *J*(C,P) 117].

***trans*-[RhI(CO)(P*i*Pr$_3$)$_2$], 14.** This compound was prepared analogously as described for **13**, using **12** (200 mg, 0.41 mmol) and NaI (285 mg, 1.9 mmol) as starting materials. Yellow crystals: yield 220 mg (93%); mp 144 °C (decomp.). Anal. found: C, 39.41; H, 7.32%. $C_{19}H_{42}IOP_2Rh$ requires: C, 39.46; H, 7.32%. NMR (C_6D_6) δ_H (400 MHz) 2.70 (6 H, m, PC*H*CH$_3$), 1.20 [36 H, dvt, *N* 16.0 *J*(H,H) 8.0, PCHC*H*$_3$]; δ_C (100.6 MHz) 187.5 [dt, *J*(Rh,C) 75.0, *J*(P,C) 14.0, CO], 26.5 (vt, *N* 10.0, P*C*HCH$_3$), 20.4 (s, PCH*C*H$_3$); δ_P (162.0 MHz) 47.6 [d, *J*(C,P) 117].

Computational details

The DFT calculations were performed using GAUSSIAN 98[36] and Becke's 1988 exchange functional[37] in combination

with the Perdew–Wang '91 gradient-corrected correlation functional (BPW91).[38] The Los Alamos effective core potential plus double zeta (LANL2DZ)[39,40] was employed for rhodium, whereas the Dunning/Huzinaga full double zeta basis set with or without polarization and diffuse function [D95, D95 + (d) and D95 + (3df, 2p) for P, C, H, F, Cl and O atoms or 6-31++G(d) for P, C, H, O, 6-311++G(d) for Br and 3-21G(d) for I] was used. The calculations were performed without symmetry restrictions. For both C_1 and C_s symmetries, very similar energies were obtained {the calculated energies for *trans*-[RhF(=C=CH_2)(PMe_3)$_2$] using the BPW91/LANL2DZ method were −593.301 98 and −593.301 01 a.u., respectively}. When C_{2v} symmetry was imposed, the rotational conformations of the phosphine groups caused difficulties in finding an energy minimum.

The following notation has been used for the computational methods used. DFT1: BPW91/LANL2DZ for all atoms; DFT2: BPW91/LANL2DZ for Rh and D95 + (d) for the other atoms; DFT3: BPW91/LANL2DZ for Rh and D95 + (3df,2p) for the other atoms; DFT4: BPW91/LANL2DZ for Rh, 6-31++G(d) for H, P, C and 6-311++G(d) for F, Cl, Br and 3-21G(d) for I.

Acknowledgements

Financial support from the Deutsche Forschungsgemeinschaft (SFB 347, projects C2 and D1) and the European Commission (Contract ERBFMBICT960698) as well as from the Fonds der Chemischen Industrie is gratefully acknowledged. We also thank Mrs R. Schedl and Mr C. P. Kneis (DTA and elemental analyses) as well as Degussa AG (gifts of various chemicals).

References and notes

1 K. Nakamoto, *Infrared and Raman Spectra of Inorganic and Coordination Compounds*, John Wiley and Sons, New York, 1986.
2 M. Tilset, J.-R. Hamon and P. Hamon, *Chem. Commun.*, 1998, 765.
3 F. Abu-Hasanayn, A. S. Goldman and K. Krogh-Jespersen, *Inorg. Chem.*, 1994, **33**, 5122.
4 A. W. Ehlers, S. Dapprich, S. F. Vyboishchikov and G. Frenking, *Organometallics*, 1996, **15**, 105.
5 L. Vaska and J. Peone, *J. Chem. Soc., Chem. Commun.*, 1971, 418.
6 H. L. M. Van Gaal and F. L. A. Van den Bekerom, *J. Organomet. Chem.*, 1977, **134**, 237.
7 S.-C. Chang, R. H. Hauge, Z. H. Kafafi, J. L. Margrave and W. E. Billups, *J. Am. Chem. Soc.*, 1988, **110**, 7975.
8 E. Diana, O. Gambino, R. Rossetti, P. L. Stanghellini, T. Albiez, W. Bernhardt and H. Vahrenkamp, *Spectrochim. Acta, Part A*, 1993, **49**, 1247.
9 C. E. Anson, N. Sheppard, D. B. Powell, J. R. Norton, W. Fischer, R. L. Keiter, B. F. G. Johnson, J. Lewis, A. K. Bhattacharrya, S. A. R. Knox and M. L. Turner, *J. Am. Chem. Soc.*, 1994, **116**, 3058.
10 E. O. Fischer, N. Q. Dao and W. R. Wagner, *Angew. Chem.*, 1978, **90**, 51; E. O. Fischer, N. Q. Dao and W. R. Wagner, *Angew. Chem., Int. Ed. Engl.*, 1978, **17**, 50.
11 G. R. Clark, K. Marsden, W. R. Roper and L. J. Wright, *J. Am. Chem. Soc.*, 1980, **102**, 6570.
12 N. Q. Dao, E. O. Fischer and T. L. Lindner, *J. Organomet. Chem.*, 1981, **209**, 323.
13 N. Q. Dao, H. Fevrier, M. Jouan, E. O. Fischer and W. Röll, *J. Organomet. Chem.*, 1984, **275**, 191.
14 J. K. Manna, R. J. Kuk, R. F. Dallinger and M. D. Hopkins, *J. Am. Chem. Soc.*, 1994, **116**, 9793.
15 M. Barnes, D. A. Gillet, A. J. Merer and G. F. Metha, *J. Chem. Phys.*, 1996, **105**, 6168.
16 R. M. Sosa, P. Gardiol and G. Beltrame, *Int. J. Quantum Chem.*, 1998, **69**, 371.
17 D. Moigno, W. Kiefer, J. Gil-Rubio and H. Werner, *J. Organomet. Chem.*, 2000, **612**, 125.
18 http://www.aist.go.jp/RIODB/SDBS/menu-e.html; IR of phenylacetylene SDBS no: 1444; CAS Registry no: 536-74-3.
19 D. M. Adams and A. Squire, *J. Chem. Soc. A*, 1968, **11**, 2817.
20 Y. S. Varshavskii, M. M. Singh and N. A. Buzina, *Zh. Neorg. Khim.*, 1971, **16**, 1372.
21 A. E. Reed, R. B. Weinstock and F. Weinhold, *J. Chem. Phys.*, 1985, **82**, 735.
22 C. Cauletti, F. Grandinetti, G. Granozzi, M. Casarin, H. Werner, J. Wolf, A. Höhn and F. J. García Alonso, *J. Organomet. Chem.*, 1990, **382**, 445.
23 (*a*) R. Brady, B. R. Flynn, G. L. Geoffroy, H. B. Gray, J. Peone and L. Vaska, *Inorg. Chem.*, 1976, **15**, 1485; (*b*) G. L. Geoffroy, H. Isci, J. Litrenti and W. R. Mason, *Inorg. Chem.*, 1977, **16**, 1950.
24 H. Kunkely and A. Vogler, *J. Organomet. Chem.*, 1999, **577**, 358.
25 Half-wave reduction potentials: (a) G. Schiavon, S. Zecch, G. Pilloni and M. Martelli, *J. Inorg. Nucl. Chem.*, 1977, **39**, 115. Equilibrium constants for halide exchange: (b) F. Araghizadeh, D. M. Branan, N. W. Hoffman, J. H. Jones, E. A. McElroy, N. C. Miller, D. L. Ramage, A. Battaglia Salazar and S. H. Young, *Inorg. Chem.*, 1988, **27**, 3752; (c) D. M. Branan, N. W. Hoffman, E. A. McElroy, N. C. Miller, D. L. Ramage, A. F. Schott and S. H. Young, *Inorg. Chem.*, 1987, **26**, 2915.
26 J. T. Poulton, M. P. Sigalas, K. Folting, W. E. Streib, O. Eisenstein and K. G. Caulton, *Inorg. Chem.*, 1994, **33**, 1476.
27 J. P. Flemming, M. C. Pilon, O. Y. Borbulevitch, M. Y. Antipin and V. V. Grushin, *Inorg. Chim. Acta*, 1998, **280**, 87.
28 K. G. Caulton, *New J. Chem.*, 1994, **18**, 25.
29 G. Frenking and N. Fröhlich, *Chem. Rev.*, 2000, **100**, 717.
30 R. Wiedemann, J. Wolf and H. Werner, *Angew. Chem.*, 1995, **107**, 1359; R. Wiedemann, J. Wolf and H. Werner, *Angew. Chem., Int. Ed. Engl.*, 1995, **34**, 1244.
31 J. Gil-Rubio, B. Weberndörfer and H. Werner, *J. Chem. Soc., Dalton Trans.*, 1999, 1437.
32 F. J. García Alonso, A. Höhn, J. Wolf, H. Otto and H. Werner, *Angew. Chem.*, 1985, **97**, 401; F. J. García Alonso, A. Höhn, J. Wolf, H. Otto and H. Werner, *Angew. Chem., Int. Ed. Engl.*, 1985, **24**, 406.
33 H. Werner, R. Wiedemann, P. Steinert and J. Wolf, *Chem. Eur. J.*, 1997, **3**, 127.
34 M. Schäfer, J. Wolf and H. Werner, *J. Organomet. Chem.*, 1995, **485**, 85.
35 C. Bussetto, A. D'Alfonso, F. Maspero, G. Perego and A. Zazzetta, *J. Chem. Soc., Dalton Trans.*, 1977, 1828.
36 M. J. Frisch, G. W. Trucks, H. B. Schlegel, P. M. Gill, W. B. G. Johnson, M. A. Robb, J. R. Cheeseman, T. Keith, G. A. Petersson, J. A. Montgomery, K. Rhaghavachari, M. A. Al-Laham, V. G. Zakrzewski, J. V. Ortiz, J. B. Foresman, J. Ciolowski, B. B. Stefanov, A. Nanayakkara, M. Challacombe, C. Y. Peng, P. Y. Ayala, W. Chen, M. W. Wong, J. L. Andres, E. S. Replogle, R. Gomberts, R. L Martin, D. J. Fox, J. S. Binkley, D. J. Defrees, J. Baker, J. P. Stewart, M. Head-Gordon, C. Gonzalez and J. A. Pople, GAUSSIAN 98, Rev. A7, Gaussian Inc., Pittsburg, PA, 1998.
37 A. D. Becke, *Phys. Rev. A: At., Mol., Opt. Phys.*, 1988, **38**, 3098.
38 J. P. Perdew and Y. Wang, *Phys. Rev. B: Condens. Matter*, 1992, **45**, 13244.
39 W. R. Wadt and P. J. Hay, *J. Chem. Phys.*, 1985, **82**, 284.
40 P. J. Hay and W. R. Wadt, *J. Chem. Phys.*, 1985, **82**, 299.
41 J. Browning, P. L. Goggin, R. J. Goodfellow, M. G. Norton, A. J. M. Rattray, B. F. Taylor and J. Mink, *J. Chem. Soc., Dalton Trans.*, 1977, 2061.
42 H. Werner, F. J. García Alonso, H. Otto and J. Wolf, *Z. Naturforsch., B: Chem. Sci.*, 1988, **43**, 722.
43 A. Wierzbicki, E. A. Salter, N. W. Hoffman, E. D. Stevens, L. Van Do, M. S. VanLoock and J. D. Madura, *J. Phys. Chem.*, 1996, **100**, 11250.
44 S. E. Boyd, L. D. Field, T. W. Hambley and M. G. Partridge, *Organometallics*, 1993, **12**, 1720.